Annals of Arid Zone 65(1): 31-51, 2026

Monthly Rainfall in Moroccan Arid Oasis Regions (1940-2017): Homogenization and Trends

Abderrazzak Sadiki, Mohamed Hanchane, Jaafar El Kassioui and Ridouane Kessabi

Department of Geography, Laboratory Territory Heritage History, FLSH Dhar El-Mehraz, Sidi Mohamed Ben Abdellah University, Fez 30000, Morocco.

Received: December 18, 2025 Accepted: March 03, 2026

Abstract: Reliable, high-quality climatic time series are essential for assessing climate change and its potential impacts, particularly in arid environments characterized by fragile natural resources, especially water resources. This study aims to perform quality control, reconstruction, and homogenization of monthly rainfall data for arid oasis basins in Morocco over the period 1940-2017. The Climatol homogenization algorithm was applied to data from local meteorological stations in order to construct a long-term, homogeneous, and coherent rainfall database suitable for climatic, hydrological, and environmental studies. Monthly rainfall trends were subsequently analysed using the non-parametric Mann-Kendall test. The results reveal contrasting trends depending on the month of the year, geographical location, and altitude. Stations located on the south-western flanks of the study area at low altitudes, exhibited increasing rainfall trends during certain months, whereas stations situated on the north-eastern flanks at higher elevations, were characterized by decreasing rainfall trends. This spatial opposition in rainfall trends is much more pronounced during the warm months, from May to August. These findings highlight the complexity of rainfall dynamics in Morocco's arid oasis regions and provide essential insights into recent precipitation variability. They constitute an important scientific basis for decision-makers and water resource managers in developing appropriate strategies for sustainable water management in the study area.

Key words: Rainfall homogenization, climatol, Mann-Kendall test, arid oasis environments, rainfall trends.

***Correspondence**
Abderrazzak Sadiki
sadiki.abderrazzak.geo@gmail.com;
mohamed.hanchane@usmba.ac.ma

Citation
Sadiki, A., Hanchane, M., El Kassioui, J., and Kessabi, R. 2026. Monthly rainfall in Moroccan arid oasis regions (1940-2017): Homogenization and trends. Annals of Arid Zone 65(1): 31-51

https://doi.org/10.56093/aaz.v65i1.174334

https://epubs.icar.org.in/index.php/AAZ/article/view/174334

Morocco, particularly its arid and sub-desert southern and south-eastern margins, is highly vulnerable to the adverse impacts of climate change (Rochdane *et al*., 2014). Located in North Africa, Morocco has coastlines along both the Atlantic Ocean and the Mediterranean Sea, extending over nearly 3,500 km (Fertah *et al*., 2017). The country covers an area of approximately 710,000 km², stretching from the Strait of Gibraltar to the southern fringes of the Sahara Desert (Almeida-Garcia and Chahine, 2015). Its climate is predominantly semi-arid but

strongly influenced by the Mediterranean Sea. Three major climatic drivers shape Morocco's climate: the Atlantic Ocean, the Mediterranean Sea, and the Sahara Desert (Born *et al.*, 2008; Ouatiki *et al.*, 2019).

The arid and sub-desert oasis regions south of the Atlas Mountains cover a large part of Morocco, where water availability mainly depends on precipitation, which is scarce and distribution irregular. In addition to snowfall over the High Atlas and Anti-Atlas mountains, water resources also depend on short-duration, high-intensity rainfall events (Sadiki and Hanchane, 2021). Assessing the spatial and temporal variability of rainfall trends in the study area is a key step for understanding potential climate change impacts, enabling decision-makers and resource managers in arid and sub-desert regions planning the climate adaptation, mitigation resilience strategies.

Climatic time series are often affected by inhomogeneities related to changes in measurement conditions (Hanchane, 2013), which may render them unrepresentative of actual climate variability. Therefore, the analysis of precipitation variability requires the use of previously homogenized time series (Brunet *et al.*, 2006); otherwise, the examination of raw rainfall data may lead to erroneous conclusions regarding natural climate variability (Coll *et al.*, 2020). Various homogenization methods have been developed depending on the climatic variable, spatio-temporal variability related to station location, length of the time series, number of missing data, availability of metadata, and density of the observation network (Aguilar *et al.*, 2003). Homogenization approaches also vary according to research objectives and methodological frameworks, reflecting the growing need for long, reliable climatic series across multiple disciplines (Beaulieu *et al.*, 2007).

Traditional homogeneity tests assess differences between neighbouring and highly correlated station series, allowing most of the climatic signal to be removed and artificial changes to be identified (Mestre and Venema, 2010). Relative homogenization methods, which assume that neighbouring stations experience similar climatic signals, are the most widely used for detecting and correcting artificial biases. Under this assumption, divergences between nearby stations may reveal inhomogeneities (Conrad and Pollak, 1950). In relative comparison tests, a candidate station's time series is compared either uniformly or against a composite reference series constructed from several nearby stations (Acquaotta and Fratianni, 2014).

Recent methods have been developed to detect inhomogeneities in climatic time series through the identification of abrupt changes (breakpoints) or short-term variations (local trends), thereby avoiding the introduction of spurious trends in climate assessments (Azorin-Molina *et al.*, 2018). Among the most widely used tools are HOMER (HOME, 2013; Mestre *et al.*, 2013), ACMANT (Domonkos, 2015; Domonkos and Coll, 2017), CLIMATOL (Guijarro, 2014, 2018), and AHOPS (Rustemeier *et al.*, 2017). HOMER is more suitable for small to medium-sized networks using metadata, whereas ACMANT, AHOPS, and CLIMATOL are particularly valuable for the automatic homogenization of large and dense networks or for ensuring uniformity in the absence of metadata. CLIMATOL offers the additional advantage of integrating metadata information within the homogenization process (Coll *et al.*, 2020).

The main objective of this study is to perform quality control, reconstruction, and homogenization of observed monthly rainfall data in Morocco's arid and sub-desert oasis regions over the period 1940-2017. The data were obtained from the Souss-Massa-Drâa, Guir-Ziz-Rhéris, and Moulouya Hydraulic Basin Agencies. To address issues of inhomogeneity, data verification, and gap filling in the rainfall records collected from 70 stations covering all arid oasis regions of Morocco, the Climatol package developed by Guijarro (2014, 2019) was applied. The study also aims to analyze trends in homogenized monthly rainfall using the Mann-Kendall Z test in order to identify stations exhibiting statistically significant increases or decreases at different significance levels (α = 1%, 5%, and 10%).

Materials and Methods

Study area

Morocco's oasis regions are located in the subtropical latitudes between 27.78°N and 33.02°N and between longitudes 1°W and

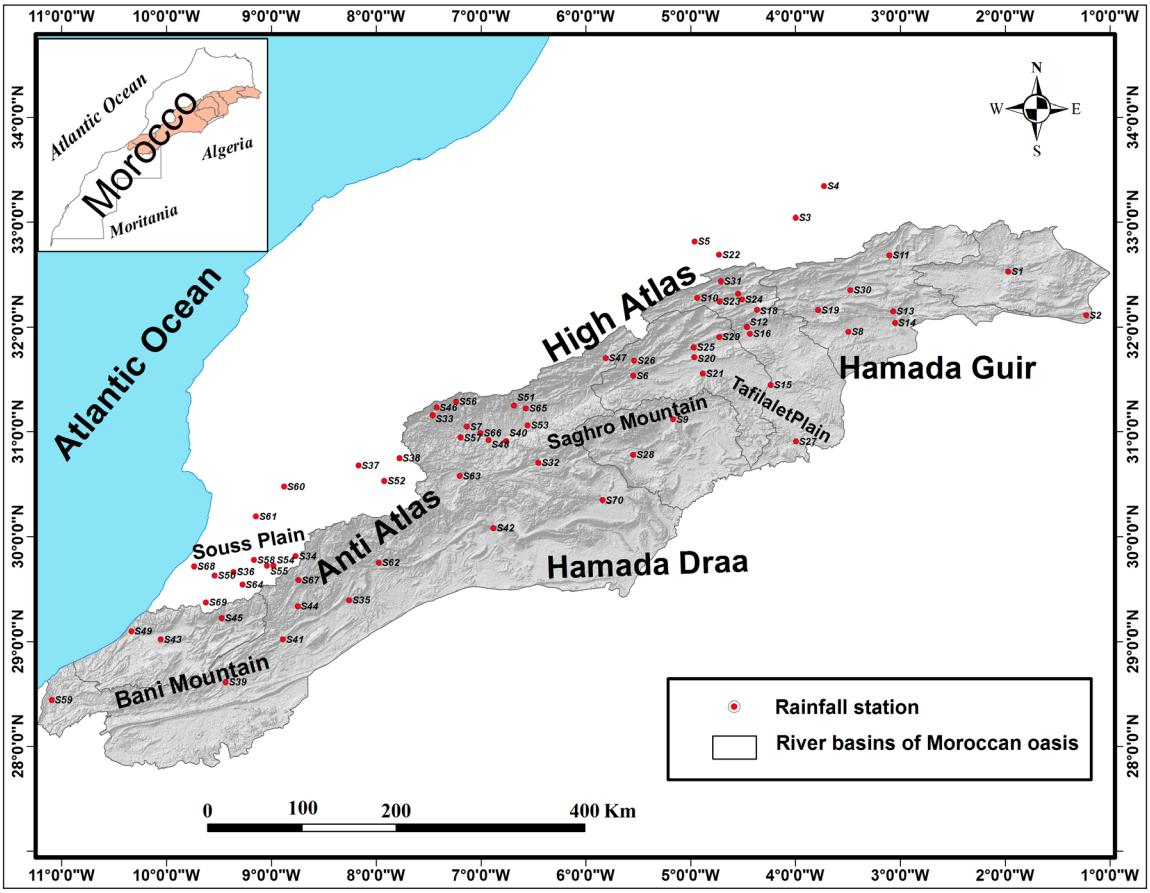

Fig.1. Geographic location of the study area and the rainfall stations.

11.02°W. These areas are dominated by the subsidence zone of the descending branch of the Hadley cell, which promotes near-permanent atmospheric stability and results in an arid to sub-desert climate. The oasis regions extend across seven river basins from east to west: Figuig, Guir, Ziz, Ghériss, Maider, Drâa, and Guelmim, covering an estimated area of 155,471 km².

The study area represents a geographical transition zone between the Mediterranean domain to the north and the Sahara Desert to the south. It is bounded to the north by the High Atlas and Anti-Atlas mountain ranges, to the east and southeast by Algeria (Guir and Drâa Hamadas), to the southeast by the Sakia El Hamra basin, and to the west by the Atlantic Ocean. This arid oasis zone, extending between the High Atlas and Anti-Atlas mountains to the north and the Sahara Desert to the south, exhibits a bioclimatic transition from mountainous environments to desert conditions. Climatic conditions are predominantly arid and desertic, largely due to the region's extensive exposure to the Sahara. Administratively, the study area spans four regions: Oriental, Drâa-Tafilalet, Souss-Massa, and Guelmim-Oued Noun, and includes eight provinces from east to west: Figuig, Errachidia, Tinghir, Zagora, Ouarzazate, Tata, Guelmim, and Assa-Zag.

Sources of observed climate data and station selection

The monthly rainfall database used in this study was collected from the Hydraulic Basin Agencies of Souss-Massa-Drâa, Guir-Ziz-Rhéris, and Moulouya (Table 1). The data set of 70 rain gauge stations of the arid oasis zones of Morocco during period of 78-years (1940-2017). The collected data series are acceptable with respect to the desired and critical thresholds required for using package of Climatol to perform homogenization; the desired threshold is indicated by the green line and the critical threshold by the red line (Fig. 2). The available data for all stations exceed the critical threshold.

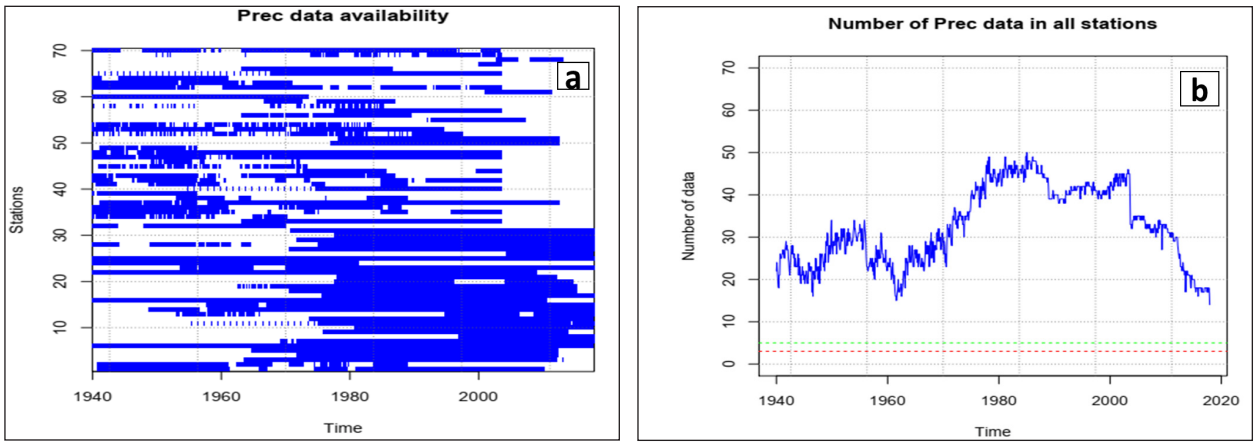

Fig. 2. (a) Rainfall database used in this study: available data are shown in blue and missing data in white; (b) Evolution of the number of observations used and data availability thresholds required by Climatol; the green and red lines indicate the desired and critical acceptance thresholds for available data, respectively.

Regarding the volume of data collected at rain gauge stations varied as temporal scale, such as a small number of stations is observed in the 1940s, followed by a marked increase since the 1960s. However, since the 2000s, a decrease in the number of observations has been noted. This overall situation raises the issue of data gaps in the available records, which will be addressed using the Climatol package in R environment, while also assessing its performance in data reconstruction and homogenization.

The Climatol package

Quality control, gap filling, and homogenization of rainfall data: Climatol (Guijarro, 2014 and 2019), developed within the R environment (R Core Team, 2015), is based on the Standard Normal Homogeneity Test (SNHT) proposed by Alexandersson (1986) and later modified by Alexandersson and Moberg (1997). It has been widely used to homogenize various climatic variables. In their analysis, Coll *et al.* (2020) concluded that Climatol's detection of inhomogeneities appeared closest to reality compared with other homogenization methods.

Climatol automates quality control and correction of outliers, homogenization (detection and correction of breaks), and infilling of missing data. It has been applied in Morocco to homogenize monthly precipitation data in different regions (Abahous *et al.*, 2020; Kessabi *et al.*, 2022a, 2022b; Addou *et al.*, 2022; Sadiki, 2023; Chanyour *et al.*, 2024). During the detection and adjustment phase, a relative homogenization approach is adopted. It assumes that precipitation amounts in a candidate series are proportional to certain regional means, as shown by Paulhus and Kohler (1952; cited by Alexandersson, 1986). This approach relies strongly on the difference series between a candidate series and its reference series. The difference series is estimated as a weighted average of the nearest and best-correlated reference series.

The homogenization procedure follows three main steps: (1) detection of inhomogeneities by applying the SNHT on overlapping windows until all series appear homogeneous; (2) detection of breaks using the SNHT applied to the entire series; and (3) gap filling using weighted ratios from neighbouring series, thereby generating the final homogeneous series.

The SNHT method has the advantage of allowing the use of nearby station data even when no common observation period exists, making it possible to include short series. To address irregular observation periods, Climatol first normalizes all original data and computes a reference series for each candidate series by averaging up to ten data series (if available) at each time step during the detection stages, and four data series during the final reconstruction stage.

For rainfall normalization, Climatol applies the ratio-to-means method, which is particularly suitable for highly skewed, L-shaped probability distributions, such as those of precipitation and wind speed. Estimates of the mean and standard deviation of the complete normalized

Table 1. Geographic description of the database and percentage of missing data

ID	Stations	Latitude (°)	Longitude (°)	Altitude (m)	Start	End	Missing data (%)
S1	Bouarfa	32.53	-1.97	1110	1940	2010	21.07
S2	Figuig	32.11	-1.22	900	1940	1989	26.53
S3	Missour	33.04	-3.99	900	1963	2012	0.85
S4	Outat Elhaj	33.34	-3.72	747	1971	2012	0.81
S5	Zaida	32.82	-4.96	1700	1964	2012	0.69
S6	Ait Boujjan	31.53	-5.54	1350	1940	2017	0.21
S7	Ait Haddou	31.05	-7.13	1300	1968	2017	4.93
S8	Akrouz	31.95	-3.49	917	1996	2017	1.58
S9	Alnif	31.12	-5.16	875	1975	2014	2.77
S10	Amouguer	32.28	-4.93	1400	1980	2017	0.67
S11	Anoual	32.68	-3.10	1203	1974	2017	1.74
S12	Barrage Hassan Addakhil	32.00	-4.46	1093	1973	2017	0.75
S13	Ben Yatti	32.15	-3.06	1029	1952	2017	54.61
S14	Bouanane	32.04	-3.05	854	1948	2017	2.89
S15	Erfoud	31.45	-4.23	823	1957	2017	2.63
S16	Errachidia	31.94	-4.43	1028	1940	2010	0.0
S17	Foum Tillicht	32.32	-4.54	1400	1975	2017	1.19
S18	Foum Zaabel	32.17	-4.52	1230	1970	2015	1.11
S19	Kaddoussa	32.16	-3.78	1300	1962	2015	6.44
S20	Lhmida	31.71	-4.95	1112	1977	2015	25.65
S21	Merroutcha	31.56	-4.52	1326	1977	2012	3.57
S22	Midelt	32.69	-4.72	1525	1940	2009	0.95
S23	Mzizel	32.24	-4.68	1441	1953	2017	8.85
S24	Rich	32.26	-4.52	1322	1939	1981	0.79
S25	Tadighoust	31.81	-4.97	1230	1940	2017	0.32
S26	Tamtoucht	31.68	-5.53	1763	2003	2017	10
S27	Taous	30.91	-3.99	693	1970	2017	0.88
S28	Tazarine	30.78	-5.54	833	1940	2017	24.78
S29	Tazouguert	31.91	-4.72	1035	1971	2017	0.54
S30	Tit N'aissa	32.35	-4.68	1369	1977	2017	0.0
S31	Z S Hamza	32.44	-4.71	1641	1970	2017	0.43
S32	Agdez	30.70	-6.45	1100	1940	1970	15.86
S33	Aguouim	31.16	-7.46	1649	1962	2003	1.42
S34	Ait Abdelah	29.81	-8.76	1750	1940	1970	42.74
S35	Akka	29.39	-8.25	350	1940	2003	45.14
S36	Anezi	29.66	-9.36	450	1940	1988	22.22
S37	Aoulouz	30.68	-8.16	700	1940	2012	6.38
S38	Askaoun	30.75	-7.77	1974	1952	1982	57.65
S39	Assa	28.61	-9.43	329	1956	1963	3.64
S40	Barrage Mansor Dahbi	30.91	-6.78	1050	1974	2003	0.28
S41	Foum El hassan	29.02	-8.89	484	1940	1983	62.41
S42	Foum Zguid	30.08	-6.88	700	1940	2003	47.88
S43	Guelmim	29.02	-10.05	300	1940	1987	16.48
S44	Ifni	29.33	-8.75	923	1971	2003	46.35
S45	Ifrane Anti Atlas	29.22	-9.47	860	1940	1973	48.23

Table 1. Cont...

ID	Stations	Latitude (°)	Longitude (°)	Altitude (m)	Start	End	Missing data (%)
S46	Ighrem	31.23	-7.42	1927	1948	1956	34.25
S47	Msemrir	31.70	-5.81	2100	1940	2003	34.65
S48	Ouarzazat	30.92	-6.96	1187	1940	2003	5.68
S49	Oued Noun	29.10	-10.33	76	1940	1956	22.39
S50	Ouijjane	29.63	-9.54	307	1976	2012	1.62
S51	Amsoul	31.25	-6.67	860	1977	2012	2.38
S52	Taliouine	30.53	-7.92	1022	1958	1997	53.65
S53	Skoura	31.06	-6.55	1220	1940	1994	12.80
S54	Tafraout	29.72	-8.98	1050	1940	1978	48.02
S55	Taguenza	29.72	-9.04	852	1992	2007	2.77
S56	Talouat	31.29	-7.23	1784	1962	1983	8.64
S57	Tamdroust	30.95	-7.19	1383	1977	2003	0.96
S58	Tanalt	29.78	-9.16	1200	1940	1985	79.81
S59	TanTan	28.44	-11.09	180	1966	1987	14.47
S60	Taroudant	30.48	-8.87	240	1940	2003	0.25
S61	Tassila	30.19	-9.14	436	2000	2011	9.48
S62	Tata	29.75	-7.97	900	1940	2003	19.84
S63	Taznakhte	30.58	-7.20	1400	1940	1971	12.09
S64	Tifermite	29.54	-9.27	1332	1943	1961	5.55
S65	Tiflite	31.22	-6.57	1450	1967	2003	0.23
S66	Tifoultoute	30.99	-6.99	1173	1962	1987	5.36
S67	Tililte	29.58	-8.74	1788	1999	2003	12.5
S68	Tiznite	29.71	-9.73	212	2002	2013	24.24
S69	Tnin Ait Irka	29.37	-9.62	1146	1973	2003	42.22
S70	Zagora	30.35	-5.84	730	1971	2003	21.95

time series (including missing values) are not computed over the entire study period when the time series is incomplete. An iterative approach is therefore used to estimate these statistics until the maximum variation between means of any data element in consecutive iterations falls below a given threshold.

Finally, Climatol generates the final homogeneous series by filling all missing data (including data removed during outlier detection and break detection) with estimated values derived from neighbouring stations. The estimated series are also used to compute the root mean square errors (RMSE) of Climatol estimates, which can serve to derive confidence intervals for the homogenized series. Anomaly series are also calculated for outlier and break detection.

The SNHT statistic is a measure of series heterogeneity: the lower the maximum SNHT value for a series, the higher its homogeneity. Climatol computes SNHT values for all series and retains the maximum SNHT value for each one. Series with maximum SNHT values exceeding a predefined threshold are split into two sub-series at the point of maximum SNHT. The sub-series are then retested, and the procedure is repeated until all maximum SNHT values fall below the specified threshold.

The Mann-Kendall Z test : Following homogenization of the collected data using R software, the Mann-Kendall Z test was applied to analyze monthly precipitation trends for each of the 70 stations considered. This non-parametric test allows the assessment of increasing or decreasing trends in precipitation time series.

The Mann-Kendall (MK) test is among the most frequently used non-parametric analyses worldwide to characterize trends in hydrometeorological time series, as proposed by Mann (1945) and Kendall and Stuart (1977). In principle, each time series is treated as an ordered sequence. Each data point is compared

with subsequent points in the series. The initial value of the S statistic is set to zero, indicating no detected trend. It is then incremented by +1 or decremented by −1. The sum of all increments and decrements yields the final S value. A large non-zero S value indicates the presence of a trend.

To assess the statistical significance of the trend, the probability associated with S and the sample size n is computed using the Z statistic, which follows a normal distribution with mean 0 and standard deviation 1. The null hypothesis is rejected if the probability exceeds the significance level α% (Hanchane, 2013). Compared with the least-squares linear regression approach, the MK test is robust to outliers and extreme values (Kessabi *et al*., 2022b). It is non-parametric (making no assumption about the underlying data distribution) and is recommended by the World Meteorological Organization (WMO).

The MK test statistic and the sign function are computed using the following formulation:

$$S = \sum_{i=1}^{n-1} \sum_{j=i+1}^{n} \operatorname{sgn}(x_j - x_i)$$

where n is the number of observations, and x represents the data values at times i and j (j > i). The variance of S is given by:

$$\operatorname{sgn}(x_j - x_i) = \begin{cases} +1, \text{if} x_j - x_i > 0 \\ 0, \text{if} x_{j-x_i=0} - 1, \text{if} x_j - x_i < 0 \end{cases}$$

The variance (V) is calculated as follows:

$$V(s) = \frac{n(n-1)(2n+5) - \sum_{k=1}^{m} t_k(t_k-1)(2t_k+5)}{18}$$

where ti is the number of ties of extent i and m is the number of tied groups. For n > 10, the standardized test statistic Z is computed as:

$$Z = \begin{cases} \frac{S-1}{\sqrt{VAR(S)}} & if \quad S > 0 \\ 0 & if \quad S = 0 \\ \frac{S+1}{\sqrt{VAR(S)}} & if \quad S < 0 \end{cases}$$

Positive Z values indicate increasing trends, while negative values indicate decreasing trends. Trend significance is assessed based on a chosen significance level α. When |Z| exceeds Z1−α/2, the null hypothesis is rejected and a significant trend is present in the time series. Z1−α/2 is obtained from the standard normal distribution table (Douglas *et al*., 2000).

In this study, the selected significance levels are α = 0.01 (99% confidence), α = 0.05 (95% confidence), and α = 0.1 (90% confidence). The presence of a statistically significant trend is evaluated using the Z value.

Results and Discussion

Homogenization of monthly rainfall

After data reading, Climatol was first run in exploratory mode using the raw rainfall data. In this mode, the first two homogenization detection steps are essentially skipped, and only anomalies of all original series are displayed. The results of this exploratory step were used to define and adjust the default threshold values applied in this mode, in order to perform a second homogenization whose results are presented in this study.

*Data verification and outlier detection***:** Monthly precipitation recorded at arid and semi-desert stations in Moroccan oasis zones rarely exceeds 50 mm, and rainfall amounts below 20 mm are predominant (Fig. 3a). Rainfall totals exceeding 100 mm are very rare. After data normalization, a threshold is set based on the deviation of normalized data relative to a fixed standard deviation threshold. This threshold is adjusted according to the number of detected outliers and the symmetry of the anomaly histogram (Fig. 3b). In this study, the threshold was set to ±5, and original data values falling outside this interval were therefore corrected.

*Selection of the SNHT threshold***:** Histograms of maximum SNHT values were used to determine the most appropriate threshold for detecting shifts in the mean of the precipitation time series. Two types of histograms were analyzed: those derived from staggered sub-periods (*snht1*) and those calculated over the entire series (*snht2*).

In general, these histograms display a high frequency of low SNHT values corresponding to relatively homogeneous series, along with one or more secondary groups characterized by higher SNHT values, which indicate the presence of inhomogeneities. A local minimum separating these groups can therefore be used to define a suitable SNHT threshold for the detection steps.

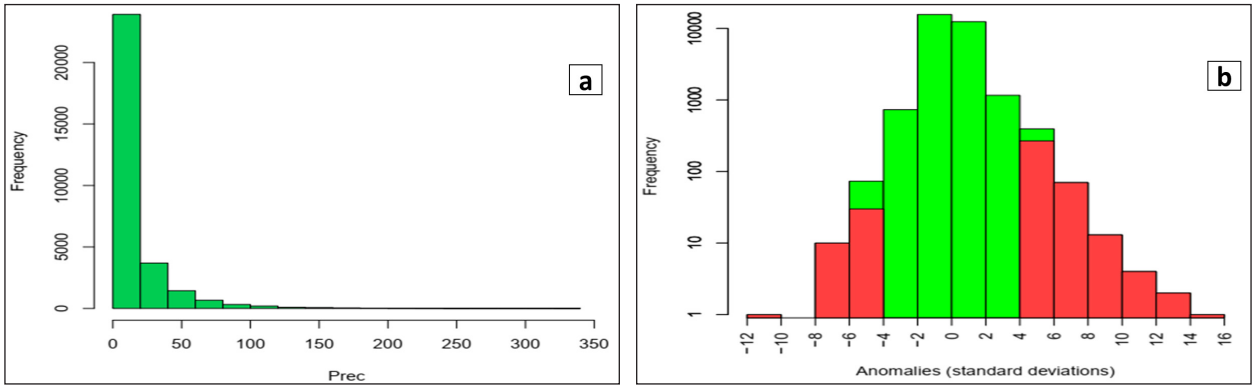

Fig. 3. (a) Frequency histogram of precipitation amounts recorded at all rainfall stations; (b) Histogram of normalized anomalies obtained during the exploratory run of the Climatol package. The x-axis represents standard deviations. Red bars indicate anomalies exceeding the default threshold of ±5 standard deviations.

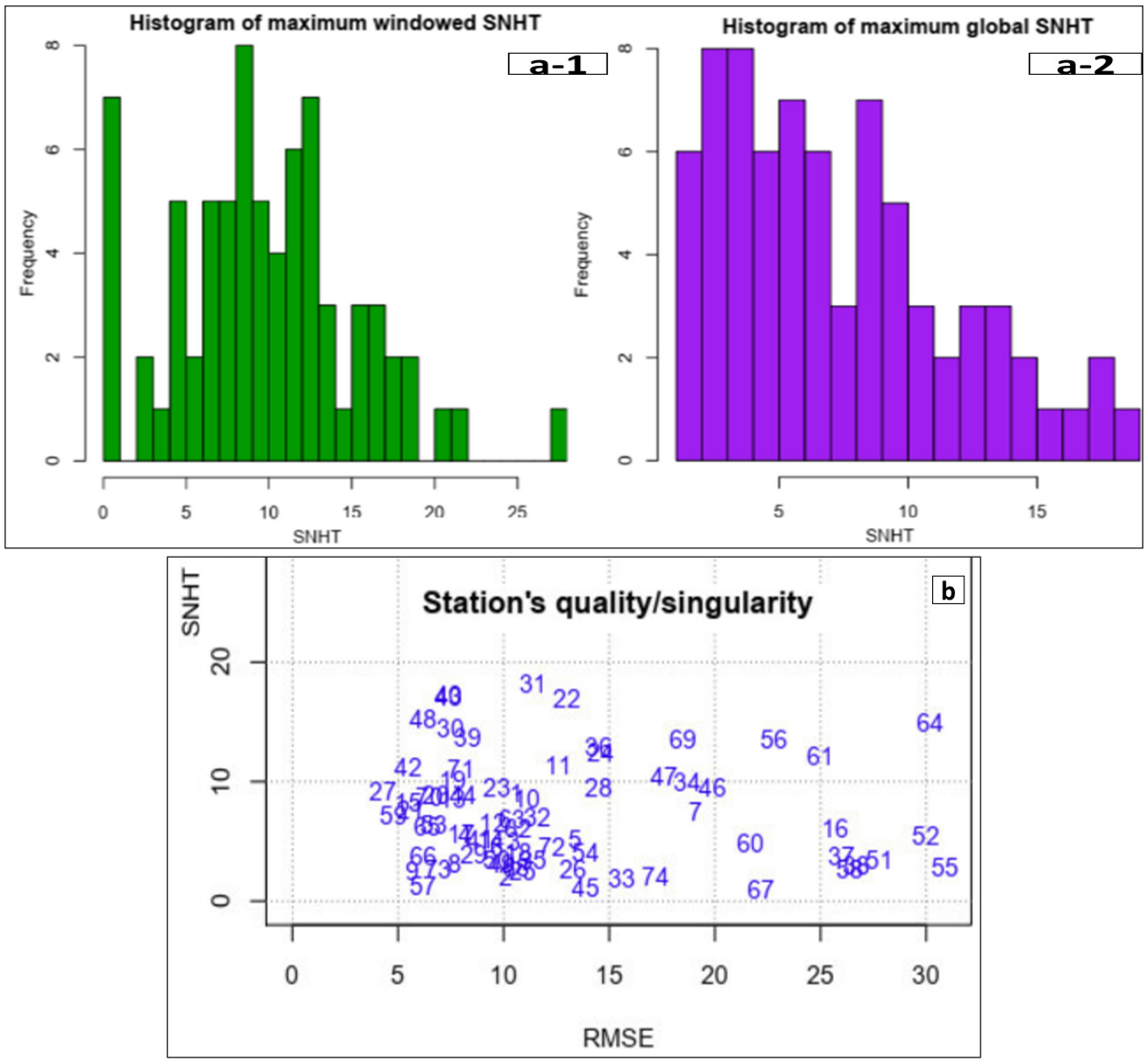

Fig. 4. (a-1) Histograms of maximum SNHT values computed over staggered windows; (a-2) Histograms of maximum SNHT values computed over the entire time series; (b) Maximum SNHT values plotted against RMSE for all stations within the study area.

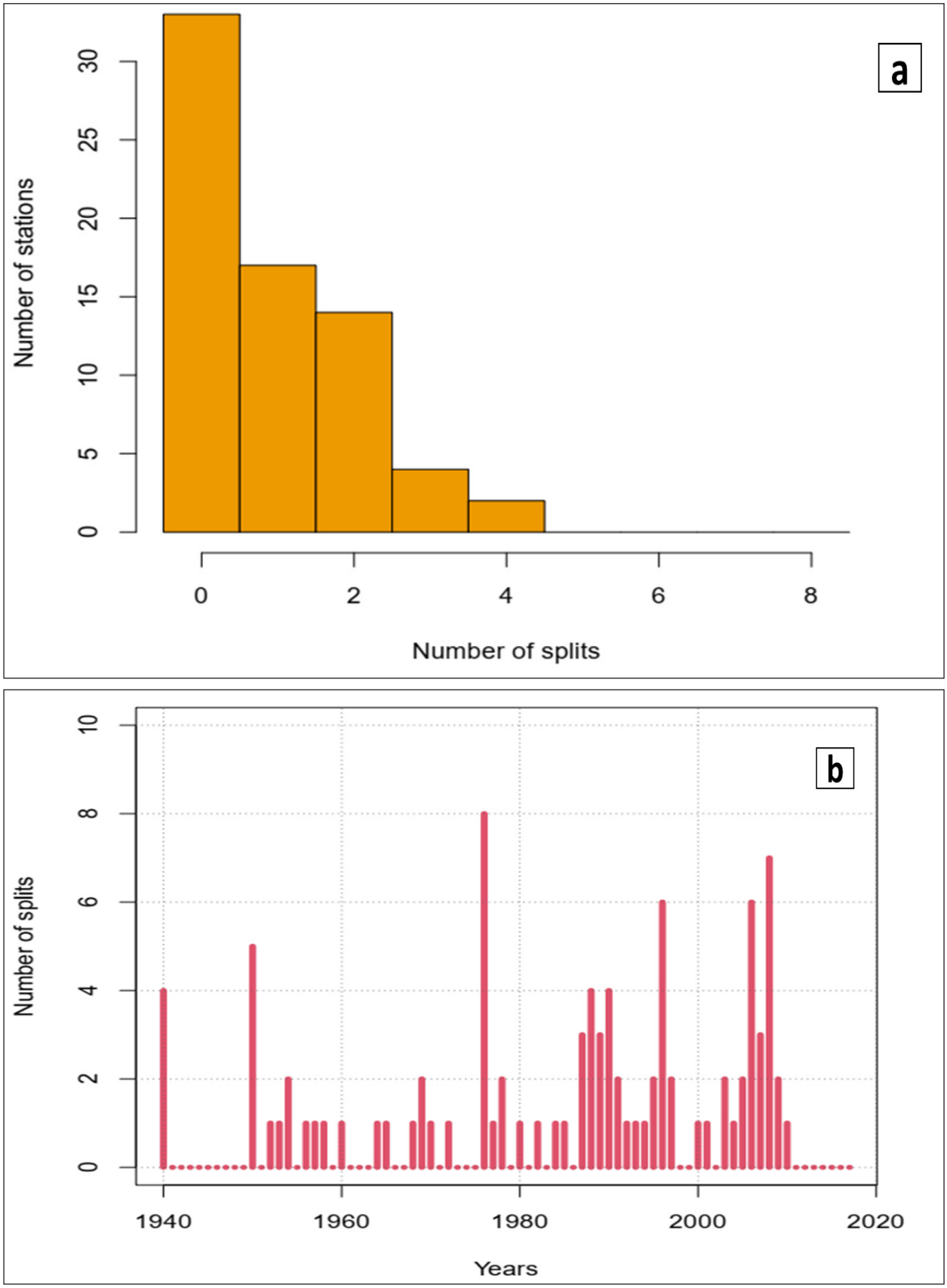

Fig. 5. (a) Histograms of the number of breakpoints (splits) per station; (b) the number of breakpoints per year.

In this study, threshold values of 12 for snht1 and 16 for snht2 were found to be appropriate, as a clear secondary group of bars separated by a marked minimum beyond higher SNHT values was observed (Fig. 4a). Figure 4b presents the final values of the root mean square error (RMSE) and the maximum SNHT values obtained after homogenization.

Breakpoint detection: Using the *Climatol* package, 94 breakpoints were detected in the precipitation time series of the Moroccan oasian rainfall observation network. As a result, 11.2% of the 70 stations were classified as non-homogeneous. In contrast, no inhomogeneities were detected in 35 out of the 70 stations (Fig. 5a).

The maximum number of breakpoints identified at a single station was four, although most stations exhibited one to two breakpoints. Analysis of the annual distribution of detected breakpoints (Fig. 5b) shows that the highest number occurred in 1976 (eight breakpoints), followed by 2008 (seven breakpoints). A closer inspection revealed that these breakpoints corresponded to the stations of Bouarfa (S1) (one breakpoint), Foum Zaabel (S18) (two breakpoints), Kaddoussa (S19) (two breakpoints), Midelt (S22) (two breakpoints), and Taous (S27) (one breakpoint).

Breakpoints numbering two or more were mainly detected from 1987 onward. In addition, single-year breakpoints were the most frequent, occurring 23 times across the dataset.

Breakpoint adjustment and reconstruction of the time series

In the absence of metadata, the acceptance of detected breakpoints was based on very high SNHT values. The example shown in Figure 6 for the Zaouiate Sidi Hamza station

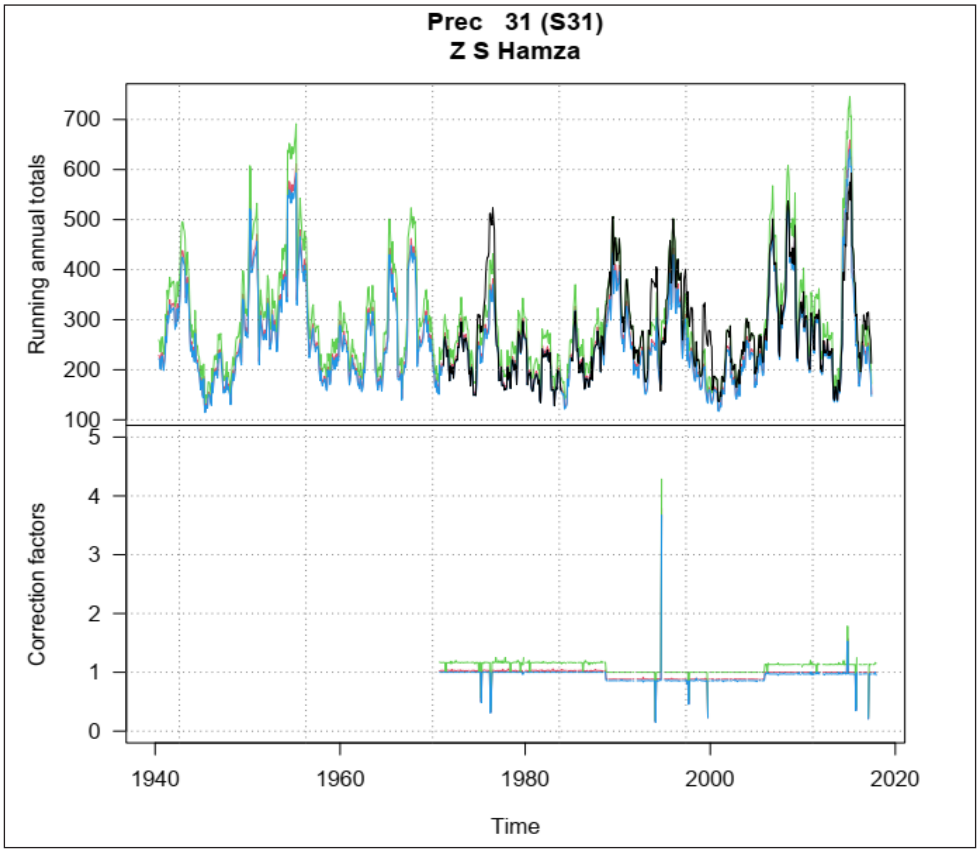

Fig. 6. Example of precipitation time-series reconstruction (top) and correction factors (bottom) at the Zaouiate Sidi Hamza station. The black line represents the original series. The red series is adjusted using the last homogeneous sub-period (2005-2017, i.e., the period after the second breakpoint) as the reference level, meaning that the rest of the series is adjusted relative to this level. The green line uses the median sub-period (2001-2011, the period between the first and second breakpoints) as the reference level, while the blue line uses the first sub-period (1972-1988, the period prior to the first breakpoint) as the reference level.

illustrates the occurrence of "peaks" resulting from the rejection of outlier values. *Climatol* provides several options for reconstructing homogenized time series. In this study, the homogenized series were reconstructed using the last homogeneous sub-period as a reference. Precipitation series were adjusted using a single annual correction factor within each homogeneous sub-period.

Normalization of precipitation data is performed only when the time series is complete. After several iterations—until the maximum variation between the means of any data element falls below a predefined threshold—the estimated means and standard deviations are used for normalization. Each term of the complete normalized raw dataset can then be reconstructed using a weighted average of a prescribed number of normalized reference series. Weighting is applied during the final reconstruction of all homogeneous sub-period series (Step 3). The reference series are weighted using an inverse distance function (Fig. 7).

In exploratory mode, using raw data, Climatol generates a correlogram that reveals correlations decreasing with distance and even becoming negative in some cases (Fig. 7b). After homogenization, correlations become entirely positive and stabilize beyond a distance of approximately 400 km, after which they appear to be independent of distance. In addition, a small number of stations exhibit a decrease in correlation with distance that stabilizes at around 200 km.

Most stations in the first group, located within a maximum distance of 400 km, show correlation coefficients greater than 0.5, whereas the second group includes stations with correlations ranging between 0.4 and 0.2 over distances up to 200 km. Given the highly variable topography of the study area, mountain stations generally exhibit weaker correlations over shorter distances (<200 km) compared to lowland stations. These orographic discontinuities may lead to contrasting precipitation regimes: mountainous areas exposed to Atlantic influences receive higher precipitation amounts, whereas more continental and eastern regions are considerably drier.

Climatol generates the final homogenized series by filling all missing data—including values removed during outlier detection and breakpoint identification—using estimates derived from neighboring stations. The reconstructed series are also used to compute root mean square errors (RMSE) of the *Climatol* estimates, which can serve to derive confidence intervals for the homogenized time series. Anomaly series are also computed for both outlier and breakpoint detection.

The SNHT statistic provides a quantitative measure of time-series heterogeneity: the lower the maximum SNHT value, the higher the degree of homogeneity. *Climatol* computes

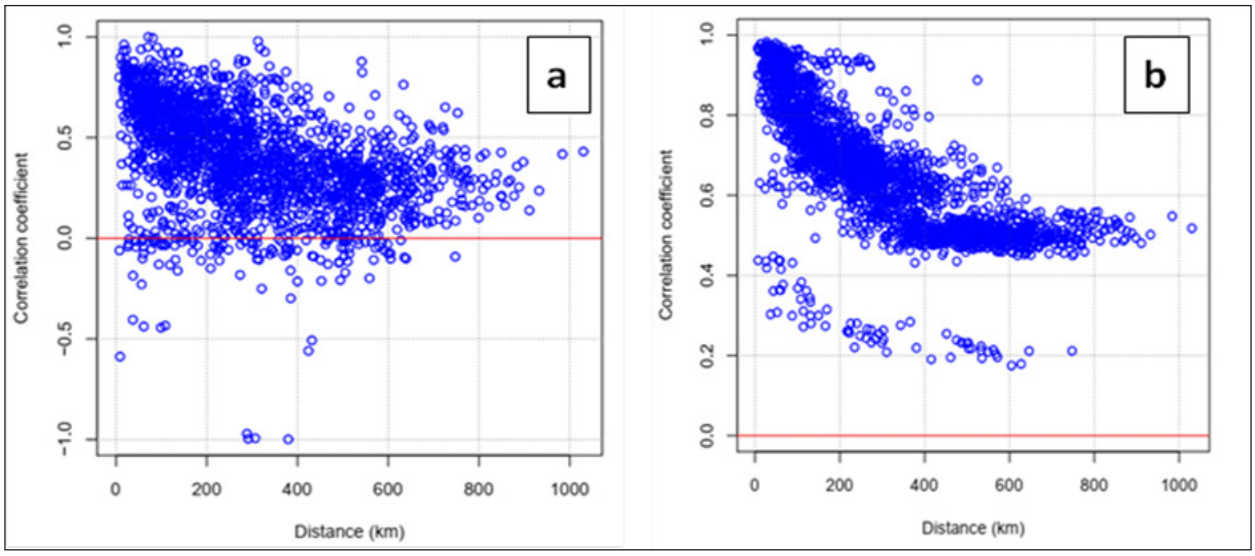

Fig. 7. Correlograms of the first differences of station time series: (a) raw data and (b) homogenized data.

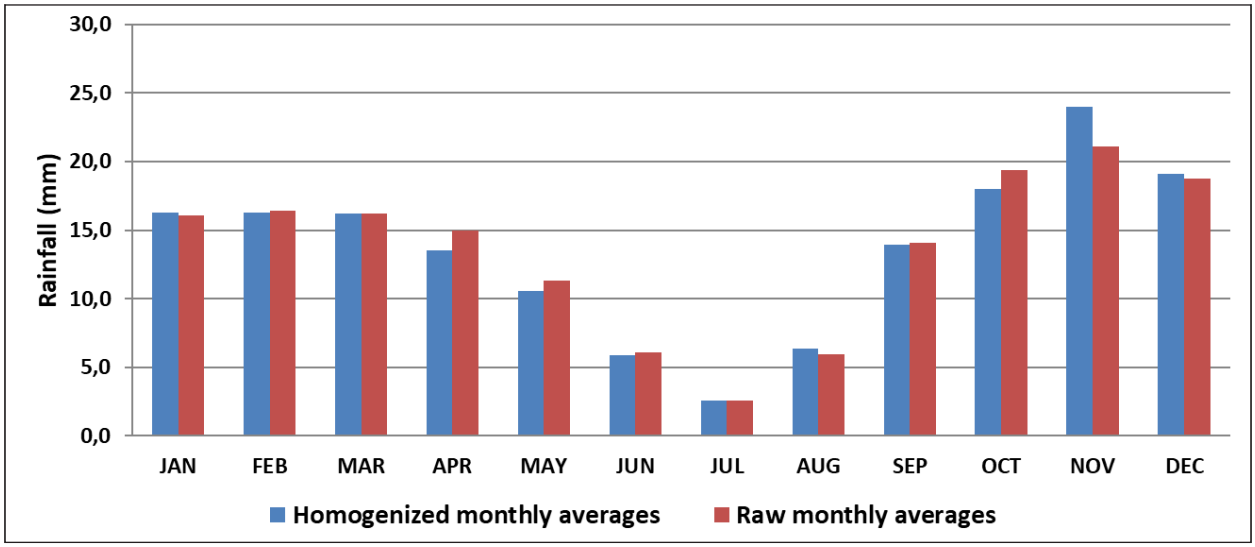

Fig. 8. Monthly means of raw and homogenized precipitation data for the study area.

SNHT values for all series and retains the maximum SNHT value for each one. The results indicate that most of the analyzed series fall within an SNHT range below 20, with RMSE values between 5 and 30 mm (Fig. 4b).

After homogenizing the monthly precipitation data, a comparison was carried out between the monthly means of the raw series and those of the homogenized series. Climatol proved effective in reconstructing missing data, detecting and removing outliers, and adjusting the homogenized series so as to represent the monthly precipitation regime in the arid oasis regions of Morocco, for all station types combined (mountain stations, hammadas—desert plateaus—plains, valleys, and the Atlantic coast) (Fig. 8).

The analysis of monthly means shows that the absolute difference between the monthly average values of the two datasets, raw and homogenized, does not exceed a maximum of 2.9 mm in November, 1.5 mm in April, and 1.4 mm in October (Fig. 8). This confirms the effectiveness of the homogenization process carried out using Climatol, as also demonstrated in several previous studies (Curci *et al.*, 2021; Guijarro, 2018; Abahous *et al.*, 2020; Kessabi *et al.*, 2022; Addou *et al.*, 2022; Sadiki, 2023).

Analysis of monthly precipitation trends: Once climatic time series have undergone processing to correct for inhomogeneities related to observation conditions (Brunetti *et al.*, 2006; Ribeiro *et al.*, 2016), they can be used to obtain an accurate picture of the state of the climate and its trends in the target area (Peel *et al.*, 2007; Brunetti *et al.*, 2014).

The application of the Mann-Kendall test to the monthly precipitation series from the 70 stations over a 78-year period (1940-2017) reveals both significant increasing and decreasing trends that vary according to the month of the year (Tables 2 and 3, and Fig. 9), as well as numerous non-significant trends.

The analysis of monthly precipitation trends in oasis stations highlights a marked seasonal variability, dominated by changes that are mostly not statistically significant.

December stands out with a generalized decreasing trend in precipitation observed at the majority of stations. However, this decrease is statistically significant for only 44.3% of the stations, while 55.7% show a non-significant decline.

A decreasing precipitation trend is also observed in November, January, and April, but it remains largely non-significant, with only a limited proportion of stations exhibiting statistically significant trends (5.7%, 14.3%, and 18.6%, respectively). From October onward, an increase in precipitation is observed at most stations (71.4%), although this increase is generally not statistically significant. The first significant increases are detected as early as September (4.3% of stations), then become more frequent during the summer months (June to August), indicating a relative intensification of summer precipitation. This dynamic weakens in May before strengthening again in March,

Table 2. Monthly rainfall trends for each station

ID	*Jan*	*Feb*	*Mar*	*Apr*	*May*	*Jun*	*Jul*	*Aug*	*Sep*	*Oct*	*Nov*	*Dec*
S1	-1.71***	-0.28	-1.35	-1.37	-0.89	-0.25	1.09	0.52	0.19	0.48	-0.52	-2.82*
S2	-0.61	-0.21	-0.53	-0.78	0.63	0.56	2.79*	2.21**	1.20	0.55	0.15	-1.82***
S3	-2.50**	-0.03	0.09	-0.87	0.29	-1.51	-1.21	0.30	0.99	0.22	-1.32	-2.85*
S4	-2.83*	-0.85	-0.18	-1.02	0.60	-1.57	-1.87***	0.41	0.27	0.30	-0.83	-3.74*
S5	-1.05	1.29	-0.04	-1.20	-1.62	-1.16	-0.54	0.88	-0.94	-0.28	-1.08	-1.48
S6	0.05	1.19	3.09*	-0.06	-0.46	2.33**	4.03*	3.55*	0.57	1.12	-0.82	-1.77***
S7	-0.76	1.53	1.32	-0.07	1.33	1.00	-1.34	-1.57	-0.05	0.56	-1.30	-1.46
S8	-1.30	-0.18	0.20	-1.93***	-1.79***	-3.85*	-5.29*	-2.67*	-0.54	-0.28	-2.06**	-4.19*
S9	-1.22	0.60	0.93	-1.54	-1.24	-0.24	1.40	1.29	-0.64	0.98	-1.08	-2.38**
S10	-2.17**	0.09	1.49	-2.16**	-2.19**	-1.85***	-3.70*	1.62	1.25	-0.07	-1.76***	-4.04*
S11	-2.26**	-1.78***	-2.06**	-2.95*	-1.61	-1.85***	-4.27*	-1.90***	-0.94	-0.90	-0.20	-3.62*
S12	-0.85	0.43	-0.18	-2.02**	-3.15*	-3.09*	-3.57*	-2.18**	-0.93	-0.51	-1.37	-2.24**
S13	-1.30	-1.22	-1.78***	-1.25	-2.42**	-3.69*	-2.38**	-3.57*	-0.53	-0.10	0.00	-2.26**
S14	-0.59	-0.72	-1.13	-1.82***	-1.66***	-0.87	-1.54	-0.27	-0.38	0.44	0.05	-2.06**
S15	-0.90	0.65	-0.19	-1.29	-2.87*	-1.38	-1.88***	-0.41	-0.42	0.45	-1.27	-2.68*
S16	-0.94	0.65	3.40*	1.45	-0.82	0.98	-0.37	-1.39	0.96	1.53	-0.40	-1.21
S17	-1.46	0.79	1.59	-1.57	-1.55	-0.94	-0.90	0.61	0.51	0.43	-1.95***	-3.12*
S18	-1.27	0.82	1.03	-1.38	-2.08**	-2.33**	-2.02**	0.28	-0.22	0.50	-1.27	-2.88*
S19	-1.20	-0.19	-0.71	-2.12**	-2.41**	-2.81*	-4.04*	-1.58	-1.73***	-0.62	-1.16	-2.24**
S20	-0.73	1.30	-0.77	-1.23	-2.33**	-1.00	-2.21**	-1.07	-0.30	-0.76	-1.38	-2.97*
S21	-1.10	0.31	1.20	-1.54	-2.50**	-1.13	-2.32**	-0.82	-0.70	0.16	-1.95***	-2.96*
S22	-1.04	0.29	1.01	-1.89***	-0.48	-1.11	0.85	3.24*	1.12	0.80	-0.73	-2.13**
S23	-0.94	0.43	1.79***	-1.65***	-1.62	-0.67	-0.92	2.17**	1.01	0.25	-1.30	-2.83*
S24	0.79	1.71***	2.05**	-1.26	-0.85	1.82***	3.79*	3.83*	0.52	0.27	-0.76	-1.27
S25	-0.11	2.17*	2.27**	-0.87	-1.10	1.31	1.64	2.91*	0.40	0.39	-0.97	-1.75***
S26	-0.89	1.17	2.27**	-2.08**	-1.75***	0.96	1.97**	2.75*	-0.06	0.39	-1.47	-2.87*
S27	-1.57	-0.17	-1.12	-1.31	-2.43**	-4.30*	-3.21*	-2.73*	-2.32**	0.05	-1.58	-2.94*
S28	0.13	0.10	0.67	-2.25**	0.65	-1.79***	0.83	0.56	-1.67***	0.58	0.29	-2.55**
S29	-1.10	0.13	-0.48	-1.74***	-2.71*	-2.30**	-3.63*	-1.96**	-1.46	-0.67	-0.85	-1.79***
S30	-1.40	-0.64	-0.36	-1.78***	-2.17**	-1.97**	-2.60*	-1.39	0.01	-0.90	-0.92	-2.45**
S31	-1.39	1.12	1.17	-1.95***	-1.45	-0.36	-0.85	1.23	0.36	0.85	-1.56	-2.96*
S32	0.81	2.10*	2.60*	0.79	2.08**	3.46*	4.54*	2.80*	0.15	1.60	-0.03	0.02
S33	-0.32	1.81***	1.26	-0.54	0.48	2.43**	1.39	0.89	0.32	0.51	-0.41	-0.95
S34	-0.99	1.32	1.92***	-0.62	0.40	2.65*	2.79*	0.96	-0.06	1.62	0.50	-0.97
S35	0.52	1.49	3.83*	1.47	4.44*	4.48*	4.22*	1.64	0.21	1.43	0.95	0.33
S36	-1.76***	0.48	1.19	-0.58	0.47	2.38**	4.77*	3.62*	1.79***	2.55**	0.50	-1.14
S37	-1.04	0.15	0.80	-0.72	0.76	3.23*	1.48	2.39**	0.25	0.88	0.21	-0.74
S38	-0.40	1.20	1.48	-0.06	1.08	3.41*	1.67***	0.62	0.33	0.85	-0.06	-0.96
S39	0.50	1.89***	3.07*	1.23	3.13*	3.95*	4.06*	2.62*	-1.11	1.70***	0.43	-0.20
S40	-0.35	0.99	1.40	-0.38	-0.45	1.71*	0.75	0.55	-0.21	0.35	0.43	-1.01
S41	0.30	1.52	1.82***	0.25	1.10	3.03*	4.19*	2.76*	0.47	1.31	0.08	-0.10
S42	0.35	2.48*	2.54**	0.45	0.97	2.42*	2.10**	1.40	-0.71	0.74	-0.20	-0.75
S43	-0.09	1.23	1.80***	1.07	3.44*	4.19	4.73*	4.25*	2.85*	2.86*	-0.25	-0.73
S44	-0.99	0.72	1.59	-1.01	0.00	2.13**	2.32**	0.27	-0.64	1.10	0.50	-0.96
S45	-0.85	1.76***	1.60	0.05	0.53	2.12**	2.97*	1.28	-0.13	1.62	-0.57	-0.66

Table 2. Cont...

ID	*Jan*	*Feb*	*Mar*	*Apr*	*May*	*Jun*	*Jul*	*Aug*	*Sep*	*Oct*	*Nov*	*Dec*
S46	-0.18	1.56	1.78***	-0.29	1.27	2.82*	2.78*	1.27	-0.03	0.57	-0.68	-0.79
S47	-0.82	1.46	1.25	-1.53	-0.36	1.54	2.99*	2.43**	0.28	1.00	-0.64	-1.99**
S48	0.52	1.80***	2.03**	-0.50	0.58	2.48**	0.17	0.40	-0.23	0.73	-0.81	-0.56
S49	-1.67***	1.12	1.89***	-0.42	0.92	3.05*	3.09*	3.58*	0.43	1.98**	0.42	-1.62
S50	-1.49	0.20	0.79	-1.09	-1.93***	0.41	0.01	-0.79	-1.74	0.76	-0.59	-1.89***
S51	-1.71***	-0.28	-1.35	-1.37	-0.89	-0.25	1.09	0.52	0.19	0.48	-0.52	-2.82*
S52	-0.49	0.57	0.89	-0.92	1.14	3.25*	2.04**	0.02	0.26	1.29	-0.25	-1.05
S53	0.72	2.45*	1.96**	-0.45	1.22	2.95*	2.42**	2.32**	-0.18	0.58	-0.12	-0.31
S54	-1.33	0.50	1.44	-0.46	0.04	1.43	2.04**	0.65	-0.82	1.59	0.08	-0.86
S55	-1.70***	0.11	1.15	-1.11	-0.61	1.15	1.24	-0.80	-0.95	1.11	0.09	-0.97
S56	-0.38	1.78***	1.58	-0.26	0.96	2.48**	1.39	0.67	-0.17	0.62	-0.72	-0.63
S57	-0.10	1.29	1.28	-0.88	-0.29	1.71***	-0.37	-0.33	-0.29	0.25	-0.78	-0.46
S58	-1.59	0.51	0.88	-0.60	-0.06	2.15**	2.32**	1.21	0.11	1.75***	0.06	-1.24
S59	-1.25	0.93	1.67***	-0.44	0.29	2.70*	2.94*	1.71***	-0.15	1.68***	-0.56	-1.46
S60	-1.26	-0.07	0.99	0.67	3.23*	5.07*	5.24*	5.41*	2.99*	2.28**	0.56	-1.14
S61	-1.32	0.37	1.25	-0.33	-1.57	0.32	0.75	0.22***	-0.37	1.68***	0.25	-1.67***
S62	0.92	1.27	2.87*	0.94	2.83*	4.20*	2.72*	2.24**	0.26	1.80***	0.99	0.04
S63	0.95	2.87*	3.10*	2.07**	2.41**	4.25*	2.22**	1.23	-0.42	1.14	-0.71	0.59
S64	-1.69***	0.46	1.17	-0.48	0.11	2.72*	3.61*	2.52**	1.20	2.19**	0.18	-1.63
S65	-0.37	1.11	1.70***	-1.24	-0.26	1.45	0.92	0.27	-0.79	0.41	-0.82	0.53
S66	-0.11	1.48	2.00**	0.17	0.85	2.96*	0.43	0.50	-0.22	0.82	-0.35	-0.67
S67	-1.40	0.53	1.59	-0.95	-0.26	1.63	2.05**	-0.53	-0.32	0.91	0.16	-0.98
S68	-1.48	0.60	0.79	-0.95	-0.18	0.83	1.77***	0.49	-1.09	1.58	-0.28	-1.29
S69	-1.58	0.53	0.70	-0.98	-0.62	0.67	1.82***	0.32	-0.63	0.96	-0.36	-1.27
S70	0.05	1.09	1.97**	-0.13	1.51	2.24**	2.78*	2.04**	-0.12	1.29	-0.17	-0.47

*Trend significant at α = 0.01 (99% confidence level); **Trend significant at α = 0.05 (95% confidence level); ***Trend significant at α = 0.10 (90% confidence level).

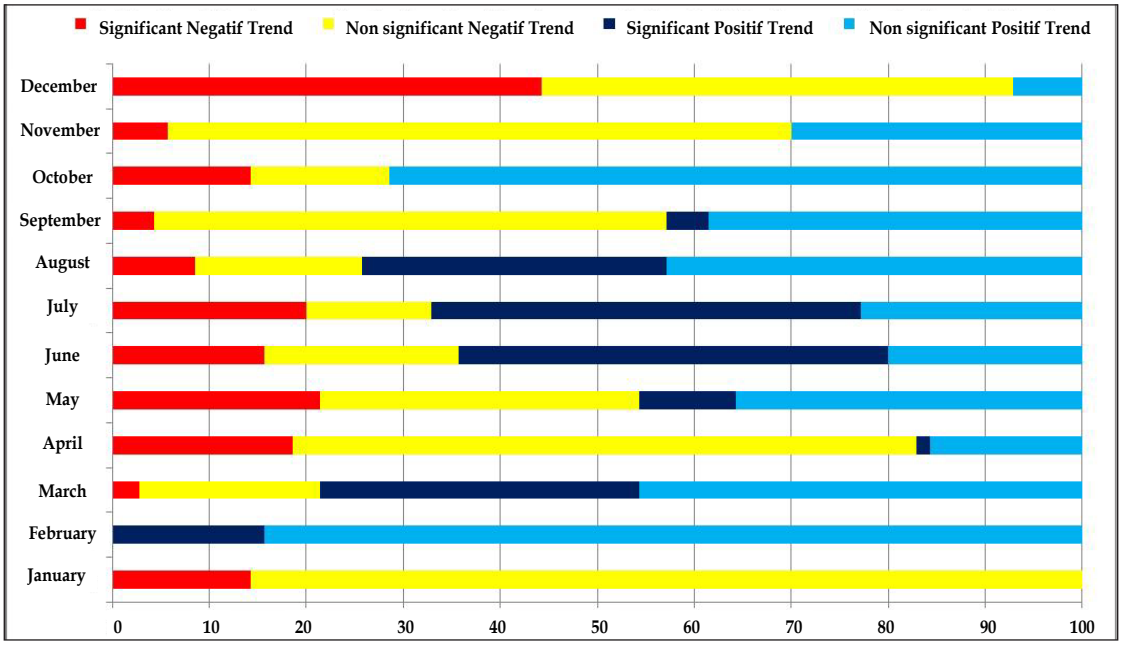

Fig. 9. Monthly distribution of trends (%).

Table 3. Number of stations showing statistically significant trends according to a thresholds for each month.

Month	*Significant positive trend*			*Significant negative trend*		
	a = 0.01	*a = 0.05*	*a = 0.1*	*a = 0.01*	*a = 0.05*	*a = 0.1*
January	-	-	-	1	3	6
February	1	4	6	-	-	-
March	7	8	8	-	-	-
April	-	1	-	1	5	7
May	5	2	-	3	8	4
June	20	9	2	5	3	3
July	19	9	3	8	3	2
August	12	8	2	3	2	1
September	2	-	1	-	1	2
October	1	4	5	-	-	-
November	-	-	-	-	1	3
December	-	-	-	16	9	6

when 32.9% of stations record a significant increase.

Finally, unlike January, February is characterized by an increasing precipitation trend, with statistical significance observed at 15.7% of the stations.

Overall, these results indicate a weak statistical robustness of the observed trends, despite a seasonal alternation between a winter decrease and a slight increase in precipitation during the summer and transitional periods.

Spatial distribution of monthly rainfall trends: The monitoring of monthly rainfall trends highlights pronounced spatial contrasts related to altitude, latitude, and longitude. The spatial variations of the Mann-Kendall Z statistic according to these three geographic factors are illustrated in Figures 10 and 11.

From an altitudinal perspective, statistically significant decreases in precipitation are mainly observed between 750 and 1,750 m during December and April. In contrast, during the warm season from May to August, these decreases are primarily concentrated between 750 and 1,400 m. Statistically significant increases, particularly evident in March, June, July, and August, involve stations distributed across a wide range of elevations. Overall, precipitation decreases mainly affect specific altitudinal belts corresponding to the meso-Mediterranean and montane Mediterranean bioclimatic zones.

Latitudinally, stations exhibiting significant decreases in precipitation occupy variable positions depending on the time of year. In January, April, and especially December, these decreases mainly affect the northernmost latitudes, between 31° and 34°N. During the warm season, however, stations experiencing declining precipitation tend to be concentrated in the central part of the study area, between 31° and 31.5°N. Conversely, stations showing statistically significant increasing trends in March, June, July, and August are distributed across a broader latitudinal band, extending from 29°N in the south to 32°N. Increases observed during other months (February, May, and October) primarily concern more southern stations. This pattern reveals a clear contrast between southern stations, generally characterized by positive trends, and more northern stations, which are more frequently affected by decreasing precipitation. This opposition is particularly pronounced during the warm months from May to August.

In terms of longitude, stations experiencing significant decreases in precipitation are preferentially located in the eastern part of the study area, between 6° and 3°W, whereas stations with significant increases are mainly situated farther west, between 11° and 5.5°W. This longitudinal contrast is especially evident during the warm season, reflecting a marked east-west differentiation across the region.

Overall, when statistically significant monthly rainfall trends are observed, they predominantly affect the meso-Mediterranean and montane Mediterranean bioclimatic zones. During the warm season in particular, these

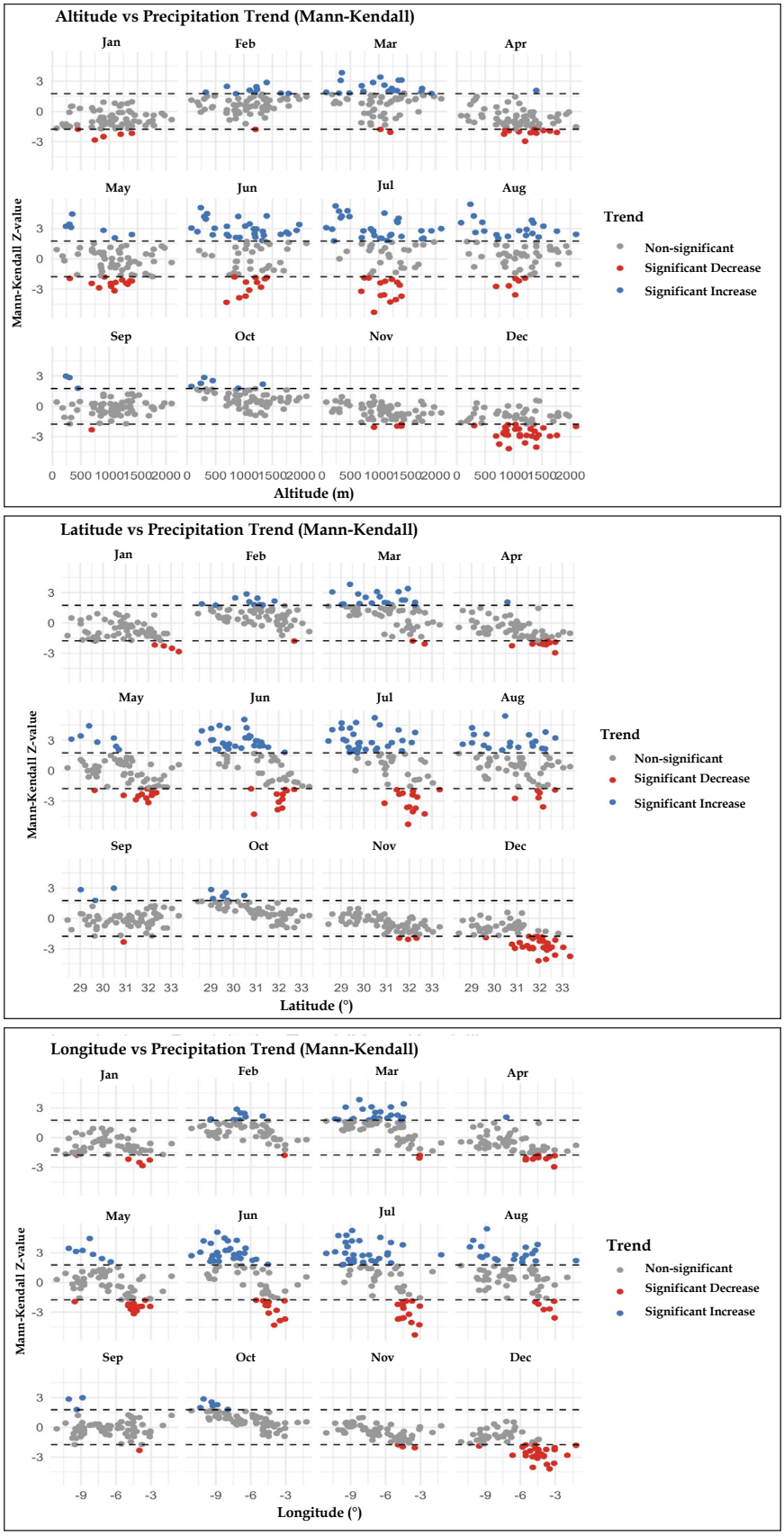

Fig. 10. Monthly variations of Mann-Kendall Z values according to altitude, latitude, and longitude.

trends oppose southern stations located in the western sector—where positive trends prevail—to more northern stations in the eastern sector, which are characterized by negative trends.

Thus, stations located on the south-western flanks of the study area, sometimes at lower elevations, have experienced increasing precipitation trends during certain months of the year, whereas stations situated on the north-eastern flanks, especially at higher elevations, are characterized by decreasing precipitation trends. This spatial contrast in rainfall trends is considerably more pronounced during the warm months from May to August. These results are illustrated in monthly distribution of Mann-Kendall Z values for all months of the year across the entire Moroccan oasian territory (Fig. 11).

Located at latitudes close to 30° N, the Moroccan oasis regions are, on average, influenced by the descending branch of the northern Hadley cell. This subsidence results in a quasi-permanent atmospheric stability and consequently explains the aridity of the environment. However, episodes of torrential rainfall may occasionally occur in the study area. Indeed, the region is sometimes affected by extreme precipitation events, which can generate major floods. This was notably the case of the 1965 flood, which devastated the Ziz Valley and led the Moroccan government to construct the Hassan Addakhil reservoir dam in 1971 upstream of the city of Errachidia (Chanyour, 2018).

In addition, the scarcity and irregularity of precipitation, combined with the succession of drought periods, have severely limited surface water resources. This situation is further exacerbated by steadily increasing anthropogenic demand (Messouli *et al.*, 2009). For example, two innovations have recently been introduced in the Todgha-Ferkla area: floodwater harvesting and the reinforcement of khettara discharge (Khardi, 2023).

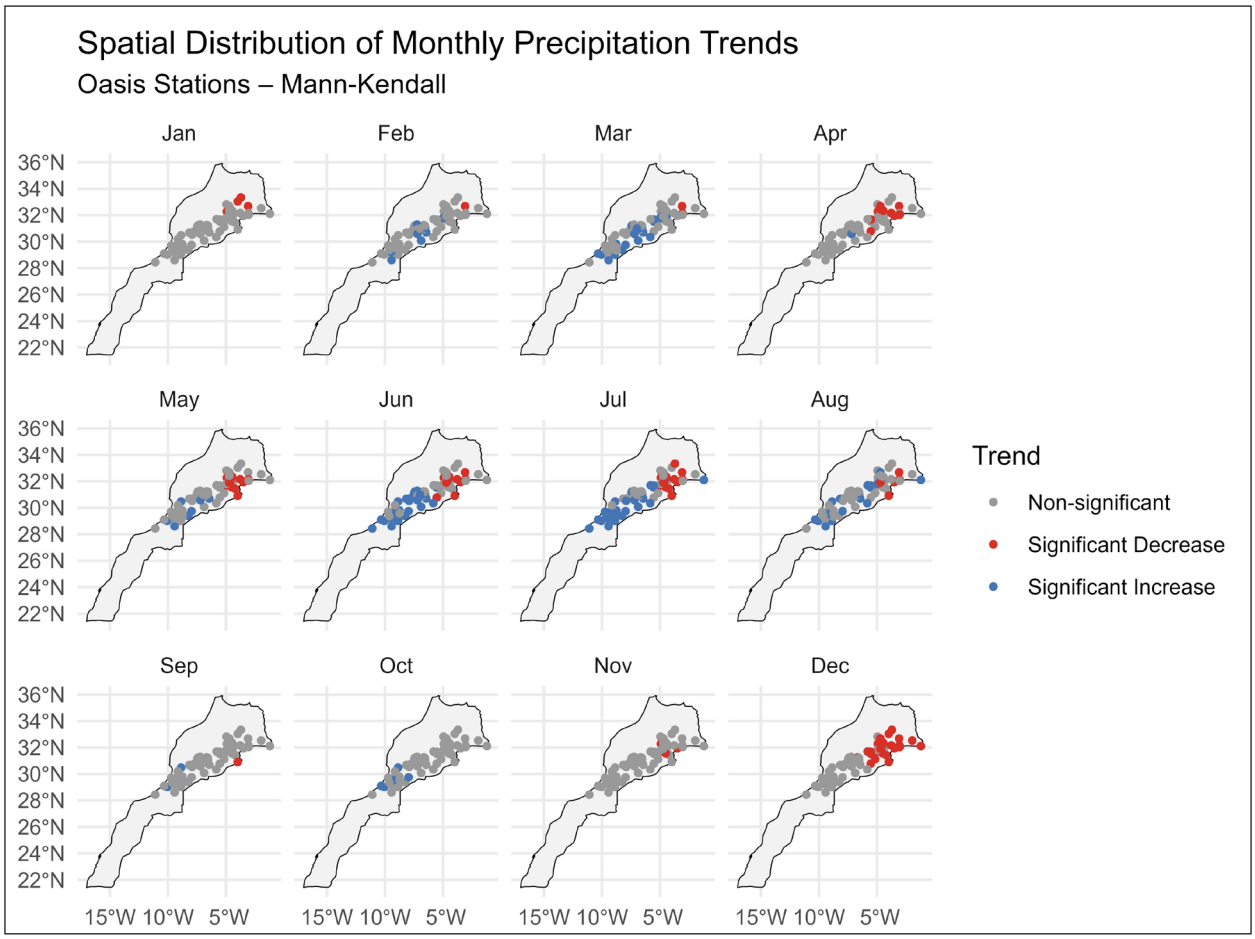

Fig. 11. Spatiotemporal distribution of Mann-Kendall Z statistics across Moroccan oasis stations.

Studies devoted to precipitation analysis in Moroccan oasis environments remain scarce and are often limited in both space and time. Yet, in order to assess vulnerability, impacts, and adaptive capacity to rainfall variability, reliable long-term time series are essential (Curci *et al*., 2021). In this study, we presented a process of quality control, reconstruction, and homogenization of monthly precipitation data covering all arid oasis regions of Morocco, using the Climatol package. After obtaining homogenized series for 70 stations, we analyzed rainfall trends over a long period from 1940 to 2017.

This work on the control and homogenization of precipitation data builds upon several previous studies conducted in Morocco (Abahous *et al*., 2020; Kessabi *et al*., 2022a, 2022b; Addou *et al*., 2022; Sadiki, 2023; Chanyour *et al*., 2024). However, the originality of our study lies in the spatial extent of the investigated area, which covers the entire Moroccan oasis territory. We thus provide a precipitation database encompassing seven major river basins: Figuig, Guir, Ziz, Ghériss, Maider, Drâa, and Guelmim. The quality of the results obtained through homogenization using Climatol is consistent with those reported in previous studies.

Homogenized precipitation series improve data quality by removing outliers likely to introduce biases in the analysis of trends and changes in rainfall variability. The analysis of monthly trends across the entire arid oasis territory of Morocco highlights contrasted evolutions, characterized by increasing or decreasing trends depending on the month and the geographical sector.

The results show that stations located on the southwestern flank of the study area, open to maritime influences and sometimes situated at low elevations, have experienced increasing precipitation trends during certain months of the year. In contrast, stations located on the northeastern flanks, particularly at higher elevations, are more strongly characterized by decreasing precipitation trends. This spatial opposition in rainfall trends is much more pronounced during the hottest months of the year, from May to August.

Studies conducted in arid regions of Algeria corroborate this decreasing precipitation tendency in the northeastern part of the Moroccan oasis territory. Hirche *et al*. (2007) emphasize that rainfall trends are sometimes difficult to identify and remain controversial, in contrast to the projections of IPCC climate models, which predict a decrease in precipitation and an intensification of aridity across the Maghreb countries (Nouaceur and Mursrescu, 2016). In continuity with our northeastern study area, the works of Hirche *et al*. (2007) and Talia *et al*. (2011) show that the arid stations located in western Algeria recorded the most pronounced decreasing precipitation trends. Indeed, no significant break was observed east of the High Plateaus and in the extreme southern Algerian Sahara, whereas the western and central High Plateaus experienced a sharp decline in rainfall.

The consistency between these results and ours suggests the existence of a decreasing southwest-northeast rainfall gradient, also affecting western Algerian stations. However, this decrease in precipitation cannot be generalized to all months of the year, nor is it uniform across the entire Moroccan oasis territory.

Thus, the analysis of rainfall trends reveals a relative increase in precipitation in oasis areas under Atlantic influence, as well as in the Drâa Basin, compared to the more continental eastern part. This eastward rainfall regression suggests a progressive limitation of the penetration of southwesterly atmospheric influences toward the east and northeast of the oasis regions—an assumption that should be further investigated and validated by future research.

Conclusions

This study highlights the spatiotemporal variability of monthly precipitation trends across all arid Moroccan oasis regions over the period 1940-2017, based on rigorously quality-controlled, reconstructed, and homogenized data series using the Climatol package. The establishment of a homogeneous database covering 70 stations and seven river basins constitutes a major methodological and scientific contribution to climate studies in Moroccan oasis environments.

The results show that precipitation trends are neither spatially uniform nor temporally constant throughout the year. A clear spatial

contrast emerges between stations located on the southwestern flanks, subject to Atlantic influences and sometimes at low elevations—where increasing precipitation trends are observed—and stations on the northeastern flank, more continental and often at higher elevations, characterized by decreasing precipitation trends. This contrast is particularly pronounced during the hot season, from May to August, a critical period for the hydrological and agro-ecological balance of oasis systems.

These findings confirm that rainfall dynamics in Moroccan oasis regions are governed by a complex combination of large-scale atmospheric drivers, topographic constraints, and continentality gradients. They also nuance global climate projections predicting a generalized decrease in precipitation over the Maghreb, by highlighting differentiated regional responses and strong seasonal contrasts.

References

Abahous, H., Guijarro, J.A., Sifeddine, A., Chehbouni, A., Ouazar, D. and Bouchaou, L. 2020. Monthly precipitations over semi-arid basins in Northern Africa: Homogenization and trends. *International Journal of Climatology* 1-11. https://doi.org/10.1002/joc.6569

Acquaotta, F. and Fratianni, S. 2014. The importance of the quality and reliability of the historical time series for the study of climate change. *Ano* 10(14): 20-38. JAN/JUL 2014.

Addou, R., Hanchane, M., Obda, K., Krakauer, N.Y., El Khazzan, B., Kessabi, R. and Achiban, H. 2022. Monthly precipitation over Northern Middle Atlas, Eastern Morocco: Homogenization and trends. *Applied Sciences* 12: 12496. https://doi.org/10.3390/app122312496

Aguilar, E., Auer, I., Brunet, M., Peterson, T.C. and Wieringa, J. 2003. Guidelines on Climate Metadata and Homogenization. Geneva: WMO, WCDMP-53, WMO-TD 1186.

Alexandersson, A. 1986. A homogeneity test applied to precipitation data. *Journal of Climatology* 6: 661-675.

Alexandersson, H. and Moberg, A. 1997. Homogenization of Swedish temperature data. 1. Homogeneity test for linear trends. *International Journal of Climatology* 17: 25-34.

Almeida-García, F. and Chahine, S. 2015. Morocco, tourism. In: *Encyclopedia of Tourism* (Eds. Jafari, J.; Xiao, H.). Academic Press. https://doi: 10.1007/978-3-319-01669-6_325-1

Azorin-Molina, C., Guijarro, J.A., McVicar, T.R., Trewin, B.C., Frost, A.J. and Chen, D. 2018. An approach to homogenize daily peak wind gusts: An application to the Australian series. *International Journal of Climatology* 39: 2260-2277. https://doi.org/10.1002/joc.5949

Beaulieu, C., Ouarda, T.B.M.J. and Seidou, O. 2007. Synthèse des techniques d'homogénéisation des séries climatiques et analyse d'applicabilité aux séries de précipitations. *Hydrological Sciences Journal* 52(1): 18-37. https://doi.org/10.1623/hysj.52.1.18

Born, K., Fink, A.H. and Paeth, H. 2008. Dry and wet periods in the northwestern Maghreb for present day and future climate conditions. *Meteorologische Zeitschrift* 17(5): 533-551. https://doi.org/10.1127/0941-2948/2008/0313

Brunet, M., Saladie, O., Jones, P., Sigro, J., Aguilar, E., Moberg, A., Lister, D., Walther, A., Lopez, D. and Almarza, C. 2006. The development of a new dataset of Spanish daily adjusted temperature series (SDATS) (1850-2003). *International Journal of Climatology* 26: 1777-1802.

Brunetti, M., Maugeri, M., Monti, F. and Nanni, T. 2006. Temperature and precipitation variability in Italy in the last two centuries from homogenised instrumental time series. *International Journal of Climatology* 26: 345-381. https://doi.org/10.1002/joc.1251

Brunetti, M., Maugeri, M., Nanni, T., Simolo, C. and Spinoni, J. 2014. High-resolution temperature climatology for Italy: interpolation method intercomparison. *International Journal of Climatology*, 34, 1278-1296. https://doi.org/10.1002/joc.3764

Chanyour, Y. 2018. Hydrologie des milieux arides et présahariens du Sud-est marocain: Cas du bassin versant de l'oued Daoura (Doctoral thesis). FLSH DM Fès, Morocco.

Chanyour, Y., El Achari, O., Hanchane, M., Obda, K. and Kessabi, R. 2024. Monthly and annual precipitation in arid environment of the Daoura watershed (South-Eastern Morocco): Homogenization and trend analysis. *Ecological Engineering and Environmental Technology* 25(4): 125-142. https://doi.org/10.12912/27197050/178530

Coll, J., Domonkos, P., Guijarro, J.A., Curley, M., Rustemeier, E., Aguilar, E., Walsh, S. and Sweeney, J. 2020. Application of homogenization methods for Ireland's monthly precipitation records: Comparison of break detection results. *International Journal of Climatology* 40: 6169-6188. https://doi.org/10.1002/joc.6575

Conrad, V. and Pollak, C. 1950. *Methods in Climatology*. Harvard University Press.

Curci, G., Guijarro, J.A., Di Antonio, L., Di Bacco, M., Di Lena, B., and Scorzini, A.R. 2021. Building a local climate reference dataset: Application to the Abruzzo region (Central Italy), 1930-2019. *International Journal of Climatology* 1-23. https://doi.org/10.1002/joc.7081

Domonkos, P. 2015. Homogenization of precipitation time series with ACMANT. *Theoretical and Applied Climatology* 122: 303-314. https://doi.org/10.1007/s00704-014-1298-5

Domonkos, P. and Coll, J. 2017. Homogenization of temperature and precipitation time series with ACMANT3: method description and efficiency tests. *International Journal of Climatology* 37: 1910-1921. https://doi.org/10.1002/joc.4822

Fertah, M., Belfkira, A., Taourirte, M. and Brouillette, F. 2017. Extraction and characterization of sodium alginate from Moroccan Laminaria digitata brown seaweed. *Arabian Journal of Chemistry*, 10, S3707-S3714. https://doi.org/10.1016/j.arabjc.2014.05.003

Guijarro, J.A. 2018. Homogenization of climatic series with Climatol Version 3.1.1. State Meteorological Agency (AEMET), Balearic Islands Office, Spain.

Guijarro, J.A. 2019. *Climate Tools* (Series Homogenization and Derived Products) Package 'climatol' Version 3.1.2.

Guijarro, J.A. 2014. User's guide to climatol: An R contributed package for homogenization of climatological series Version 2.2. State Meteorological Agency (AEMET), Balearic Islands Office, Spain.

Hanchane, M. 2013. Méthodologie de régionalisation spatio-temporelle pour une analyse des précipitations (1961-1992): application au Maroc atlantique. In *Actes du Deuxième Colloque international Eau and Climat: Regards croisés Nord/Sud* (pp. 31-39). Fès, Morocco.

Hirche, A., Boughani, A. and Salamani, M. 2007. Évolution de la pluviosité annuelle dans quelques stations arides algériennes. *Revue de la Sécheresse* 18(4): 314-320.

HOME 2013. Homepage of the COST action ES0601—Advances in homogenization methods of climate series: an integrated approach (HOME). http://www.cost.eu/COST_Actions/essem/ES0601

Kendall, M.G. and Stuart, A. 1977. *The Advanced Theory of Statistics* (Vol. 1). Publishing Co., Inc., New York Macmillan. Distribution Theory, 4th Edn.

Kessabi, R., Hanchane, M., Guijarro, J.A., Krakauer, N.Y., Addou, R., Sadiki, A. and Belmahi, M. 2022a. Homogenization and trends analysis of monthly precipitation series in the Fez-Meknes region, Morocco. *Climate* 10(5): 64. https://doi.org/10.3390/cli10050064

Kessabi, R., Hanchane, M., Krakauer, N. Y., Aboubi, I., El Kassioui, J. and El Khazzan, B. 2022b. Annual, seasonaland monthly rainfall trend analysis through non-parametric tests in Sebou River Basin (SRB), Northern Morocco. *Climate* 10(11): 170. https://doi.org/10.3390/cli10110170

Khardi, Y. 2023. Analyse des innovations de mobilisation des ressources hydriques pour faire face à la pénurie d'eau dans les oasis: cas du bassin de Todgha (Maroc). *Sciences de la Terre* (Doctoral thesis). Institut Agronomique et Vétérinaire Hassan II, Morocco.

Mann, H.B. 1945. Nonparametric tests against trend. *Econometrica* 13(3): 245-259.

Messouli, M., Ben Salem, A., Ghallabi, B., Yacoubi-Khebiza, M., Ait Boughrous, A., El Alami El Filali, A., Rochdane, S. and Hammadi, F.E. 2009. Ecohydrology and groundwater resources management under global change: A pilot study in the pre-Saharan basins of Southern Morocco. *Options Méditerranéennes* 88: 255-264.

Mestre, O., Domonkos, P., Picard, F., Auer, I., Robin, S., Lebarbier, E. *et al*. 2013. HOMER: a homogenization software—methods and applications. *Idöjárás. Quarterly Journal of the Hungarian Meteorological Service* 117(1): 47-67.

Mestre, O. and Venema, V. 2010. Homogénisation de séries climatiques. 42èmes Journées de Statistique, Marseille, France.

Nouaceur, Z. and Mursrescu, O. 2016. Rainfall variability and trend analysis of annual rainfall in North Africa. *International Journal of Atmospheric Sciences* 2016: Article ID 7230450, 12 pages. https://doi.org/10.1155/2016/7230450

Ouatiki, H., Boudhar, A., Ouhinou, A., Arioua, A., Hssaisoune, M., Bouamri, H. and Benabdelouahab, T. 2019. Trend analysis of rainfall and drought over the Oum Er-Rbia River Basin in Morocco during 1970-2010. *Arabian Journal of Geosciences* 12: 128. https://doi.org/10.1007/s12517-019-4300-9

Paulhus, J.L.H. and Kohler, M.A. 1952. Interpolation of missing precipitation records. *Monthly Weather Review* 80: 129-133. https://doi.org/10.1175/1520-0493(1952)080<0129:IOMPR>2.0.CO;2

Peel, M.C., Finlayson, B.L. and McMahon, T.A. 2007. Updated world map of the Köppen-Geiger climate classification. *Hydrology and Earth System Sciences* 11: 1633-1644. https://doi.org/10.5194/hess-11-1633-2007

Ribeiro, S., Caineta, J. and Costa, A.C. 2016. Review and discussion of homogenisation methods for climate data. *Physics and Chemistry of the Earth* 94: 167-179. https://doi.org/10.1016/j.pce.2015.08.007

Rochdane, S., Bounoua, L., Zhang, P., Imhoff, M., Messouli, M. and Yacoubi-Khebiza, M. 2014. Combining satellite data and models to assess vulnerability to climate change and its impact on food security in Morocco. *Sustainability* 6(4): 1729-1746. https://doi.org/10.3390/su6041729

Rustemeier, E., Kapala, A., Meyer-Christoffer, A., Finger, P., Schneider, U., Venema, V., Ziese, M., Simmer, C. and Becker, A. 2017. AHOPS Europe—a gridded precipitation data set from European homogenized time series. In: *9th*

Seminar for Homogenization and Quality Control in Climatological Databases (pp. 88-101). Geneva: WMO, WCDMP-85.

Sadiki, A. 2023. Les oasis marocaines entre changements climatiques et durabilité des ressources en eau (thèse de doctorat). Université Sidi Mohamed Ben Abdelah, Fès, 269 p.

Sadiki, A. and Hanchane, M. 2021. Variabilité des précipitations printanières en relation avec l'ENSO en milieux oasiens marocains. In *Actes du colloque international de l'AIC: Changement climatique, pénurie des ressources en eau, nixus eau/énergie et formes d'adaptation* (pp. 407-412). Mohammedia, Maroc.

Talia, A., Meddi, M. and Bekkoussa B.S. 2011. Étude de la variabilité de la pluviométrie dans les hauts plateaux et le Sahara algériens. *Sécheresse* 22: 149-58.

Printed in March 2026